Journal for ImmunoTherapy of Cancer

Development of anti-somatostatin receptors CAR T cells for treatment of neuroendocrine tumors

Barbara Mandriani ,[1] Eleonora Pellè,[1] Francesco Mannavola,[2] Antonio Palazzo,[3] Renè Massimiliano Marsano,[3] Giuseppe Ingravallo,[4] Gerardo Cazzato ,[4] Maria Cecilia Ramello,[5] Camillo Porta,[1,2] Jonathan Strosberg,[6] Daniel Abate-Daga,[5,6] Mauro Cives[1,2]

To cite: Mandriani B, Pellè E, Mannavola F, *et al*. Development of anti-somatostatin receptors CAR T cells for treatment of neuroendocrine tumors. *Journal for ImmunoTherapy of Cancer* 2022;**10**:e004854. doi:10.1136/jitc-2022-004854

► Additional supplemental material is published online only. To view, please visit the journal online (http://dx.doi.org/10.1136/jitc-2022-004854).

Accepted 01 June 2022

For numbered affiliations see end of article.

Correspondence to
Dr Mauro Cives;
mauro.cives@uniba.it

ABSTRACT

Background Neuroendocrine tumors (NETs) overexpress somatostatin receptors (SSTRs).

Methods We developed a second-generation, ligand-based, anti-SSTR chimeric antigen receptor (CAR) incorporating the somatostatin analog octreotide in its extracellular moiety.

Results Anti-SSTR CAR T cells exerted antitumor activity against SSTR+NET cell linesin vitro. The killing activity was highly specific, as demonstrated by the lack of CAR T cell reactivity against NET cells engineered to express mutated variants of SSTR2/5 by CRISPR/Cas9. When adoptively transferred in NSG mice, anti-SSTR CAR T cells induced significant antitumor activity against human NET xenografts. Although anti-SSTR CAR T cells could recognize the murine SSTRs as shown by their killing ability against murine NET cells, no obvious deleterious effects on SSTR-expressing organs such as the brain or the pancreas were observed in mice.

Conclusions Taken together, our results establish anti-SSTR CAR T cells as a potential candidate for early phase clinical investigations in patients with NETs. More broadly, the demonstration that a known peptide drug can direct CAR T cell targeting may streamline the potential utility of multiple peptide motifs and provide a blueprint for therapeutic applications in a variety of cancers.

WHAT IS ALREADY KNOWN ON THIS TOPIC

⇒ Neuroendocrine tumors (NETs) overexpress somatostatin receptors and somatostatin analogs as well as radiolabeled somatostatin analogs are currently used in clinical practice to control tumor progression.

WHAT THIS STUDY ADDS

⇒ We developed a second-generation chimeric antigen receptor (CAR) construct incorporating octreotide, a somatostatin analog, in the extracellular domain. Anti-SSTR CAR T cells targeting somatostatin receptors showed antitumor activity both in vitro and in vivo. Although somatostatin receptors are expressed not only by NET cells, no toxicities were observed in mice.

HOW THIS STUDY MIGHT AFFECT RESEARCH, PRACTICE, OR POLICY

⇒ Biologically active drug can be successfully used as a displayed ligand to impart target specificity to CAR T cells.

INTRODUCTION

Neuroendocrine tumors (NETs) are heterogeneous malignancies originating from the diffuse neuroendocrine system. They are characterized by a relatively indolent rate of growth and the ability to secrete a variety of hormones and vasoactive peptides.[1] Once regarded as rare, NETs constitute the second most prevalent malignancy of the gastroenteropancreatic (GEP) tract, and their incidence has been steadily increasing in the last four decades.[2] Although the therapeutic landscape of NETs has recently expanded, the prognosis of patients with advanced disease still remains poor, and new, effective therapies are needed.[1]

NETs commonly overexpress somatostatin receptors (SSTR1-5).[1] SSTRs belong to a family of G-protein coupled receptors with seven transmembrane domains, and are encoded by five highly conserved intronless genes sharing 40%–60% of homology. Different SSTR subtypes are commonly co-expressed in the same NET cell and may interact forming homodimers, heterodimers or multimers, thus leading to the activation of multiple and possibly overlapping intracellular signaling cascades.[3] The overexpression of SSTRs by NET cells is presently exploited in the clinical arena for both diagnostic and therapeutic purposes. Indeed, functional imaging studies including OctreoScan and ^{68}Ga-DOTATATE PET/CT scan can detect NET lesions by using radiolabeled SSTR ligands.[1] Both synthetic somatostatin analogs (SSAs) such as octreotide and lanreotide as

well as radiolabeled SSAs including ^{177}Lu-DOTATATE mainly target SSTR2 and SSTR5 and have shown efficacy in controlling the progression of NETs in phase III clinical trials,[4–6] being currently approved for patients with advanced GEP-NETs.

Adoptive transfer of genetically modified autologous T cells is gaining traction as one of the most promising advances in cancer immunotherapy.[7] Once isolated from patients, T cells can be manipulated ex vivo to artificially generate a specific, potent, non-MHC restricted immune response against tumor cells, and impressive outcomes have been recently recorded in clinical trials of chimeric antigen receptor (CAR) T cells targeting CD19 or B cell maturation antigen in patients with B cell malignancies.[8–12] CARs are synthetic fusion proteins consisting of an extracellular antigen-recognition domain linked to an intracellular activating domain containing CD3zeta with or without additional costimulatory modules such as CD28 or 4-1BB. The extracellular portion of the CAR is responsible for the antigen recognition capability, and is conventionally constituted by the single-chain variable fragment (scFv) of an antibody (Ab). However, innovative approaches in CAR design include the replacement of the scFv with specific ligands of receptors overexpressed by tumor cells (ligand-based CARs).[13]

Given the overexpression of SSTRs by most NETs and the lack of toxicities against SSTR-expressing organs displayed by SSAs and radiolabeled SSAs in clinical practice, we developed a second-generation, ligand-based CAR directed in its anti-SSTR specificity by the SSA octreotide. Here, we characterize the antitumor activity of anti-SSTR CAR T cells against NETs both in vitro and in vivo.

MATERIALS AND METHODS

Cell lines and primary human lymphocytes

BON1, CM and QGP1 pancreatic NET (panNET) cell lines were a gift from Dr Donadelli (University of Verona, Italy), while the CNDT2.5 intestinal NET cell line was provided by Dr Lee (MD Anderson Cancer Center, Houston, Texas, USA). The lung carcinoid H727 cell line was purchased from American Type Cell Collection (ATCC; Manassas, Virginia, USA). The RIP-Tag model-derivative MIN6 murine panNET cell line was a gift from Dr. Giorgino (University of Bari, Italy). The HAP1 chronic myelogenous leukemia cell line, known to express SSTR2/5 at very low levels, was purchased by Horizon Discovery (Cambridge, UK). All cell lines were verified at our institution as recommended (ATCC Technical Bulletin no. 8; Manassas, ATCC; 2008). All cell lines were cultured as previously described,[14] while the MIN6 and HAP1 cell lines were maintained in DMEM supplemented with 15% fetal bovine serum (FBS) and Iscove modified Dulbecco medium (IMDM) supplemented with 10% FBS, respectively. Luciferase (Luc)-expressing NET cell lines were generated by lentiviral transduction using the RediFect kit (Perkin Elmer, Waltham, Massachusetts, USA) following manufacturer's instructions. Phoenix-GP packaging cells were purchased from ATCC and cultured in DMEM with 10% FBS, 1% L-glutamine and penicillin/streptomycin. Peripheral blood mononuclear cells from healthy donors were isolated by density gradient centrifugation on Ficoll-Hypaque (Thermo Fisher Scientific, Waltham, Massachusetts, USA). Primary $CD8^+$ and $CD4^+$ T lymphocytes were sorted using immunomagnetic beads through an AUTOMacs instrument (Miltenyi Biotec, Auburn, California, USA) and cultured in AIM-V medium as described.[15]

CAR design and generation of anti-SSTR CAR T cells

We designed a second-generation CAR-like construct containing (1) two molecules of the SSA octreotide in the extracellular moiety, (2) CD8 as transmembrane domain and (3) CD3ζ and CD28 in the intracellular domain. The international patent application n. PCT/US21/35110 was filed on June 1, 2021. DNA was synthesized by IDT DNA (Coralville, Iowa, USA) using an optimization algorithm for codon usage in humans and cloned between the NcoI and NotI sites of a pMSGV1-28Z retroviral vector (insert reference PMID: 30 755 478). After transformation of Stbl3 E. Coli cells (Life Technologies, Darmstadt, Germany), ampicillin-mediated selection and Sanger sequencing of the CAR sequence, Phoenix-GP cells were transfected with the CAR-containing plasmid using Lipofectamine 3000 (Invitrogen, Carlsbad, California, USA) to produce intact retroviral particles. $CD8^+$ T cells were then doubly transduced with 1:1 dilution of viral supernatant and expanded for 2 weeks in the presence of 300 IU of human recombinant IL-2 (Miltenyi Biotec).

Droplet digital PCR

Genomic DNA from T cells or from tumor xenografts was isolated using the DNase Blood & Tissue kit (Qiagen). Droplet digital PCR (ddPCR) experiments were performed on a QX200 ddPCR system (Bio-Rad, Hercules, California, USA) according to the manufacturer's instructions. FAM-labeled CAR-specific probes were multiplexed with HEX-labeled probes targeting the myocardin-like protein 2 (MKL2) reference gene, as previously described.[16] The primers and the probes are listed in online supplemental table 1. The QuantaSoft analysis software (Bio-Rad) was used to estimate the efficiency of the CAR transduction process and to determine the degree of CAR T cell infiltration of tumor xenografts.

Western blot

Transduced and untransduced (UT) lymphocytes were subjected to Western blot (WB) to assess the presence of CAR-specific bands using a mAb targeting CD3ζ (Santa Cruz Biotechnology, cat#sc-166275). Moreover, NET cells were lysed and membrane proteins were extracted using the Mem-PER Plus Membrane Protein Extraction kit (Thermo Fisher Scientific). WB analyses were performed using Abs against SSTR2 (UMB1 clone; Abcam ab134152), SSTR5 (UMB4 clone; Abcam ab109495), Na^+K^+ATPase (Abcam, ab58475) and glyceraldehyde-3-phosphate

dehydrogenase (GAPDH (Santa Cruz, sc-32233). Protein bands were visualized using an UVITEC instrument (Cambridge, UK). The ImageQuantTL software (GE Healthcare, Little Chalfont, UK) was used for band density measurement.

Flow cytometry

Flow cytometry with anti-CD3-PE/CD8-FITC/CD4-APC Abs (BD Biosciences, San Jose, California, USA) was used to assess the purity of T cell cultures. Only cultures with $CD8^+$ or $CD4^+$ T cell purity ≥97% were employed for subsequent experiments. The membrane expression of SSTR2 and SSTR5 was evaluated using human- (R&D Systems, cat#FAB4224A; R&D Systems, cat#IC4448G) or mouse-reactive (Novus Biologicals, cat#NB300-157SS; Novus Biologicals, cat#NB100-74540) Abs targeting extracellular epitopes of these receptors after omission of cell permeabilization procedures. Unstained samples were used as negative controls. The differentiation status of transduced or UT T cells to be used for in vivo experiments was assessed immediately after isolation/transduction and the day before injection in mice (after 2 weeks of culture in the presence of IL-2) by using fluorochrome-labeled Abs targeting CD45RA, CD45RO, CD95, CD62L (Miltenyi Biotec). T cell subsets were identified as follows: T naïve (T_N): $CD45RA^+/CD45RO^-/CD95^-/CD62L^+$; T stem cell memory ($T_{SCM}$): $CD45RA^+/CD45RO^-/CD95^+/CD62L^+$; T central memory ($T_{CM}$): $CD45RA^-/CD45RO^+/CD95^+/CD62L^+$; T effector memory ($T_{EM}$): $CD45RA^-/CD45RO^+/CD95^+/CD62L^-$; T effector ($T_E$): $CD45RA^+/CD45RO^-/CD95^+/CD62L^-$. The expression of T cell exhaustion markers was investigated 1 day before adoptive transfer in mice by using fluorochrome-labeled mAbs targeting CD39, PD-1, TOX, TIGIT and CTLA4 (Invitrogen). Flow cytometry experiments were performed using a BD FACSCanto II (BD Biosciences), and analyzed using FlowJo software (Tree Star, Ashland, OR).

Confocal microscopy

NET cells were fixed in paraformaldehyde and incubated overnight at 4°C with a mouse mAb against SSTR2 (R&D Systems, cat#MAB4224) or a rabbit polyclonal Ab targeting SSTR5 (Novus Biologicals, cat#NB100-74540). Cells were then incubated at room temperature with a secondary goat anti-mouse or goat anti-rabbit FITC-conjugated Ab, as appropriate. Nuclei were counterstained by 4,6-diamidino-2-phenylindole dihydrochloride (DAPI, Sigma-Aldrich). Images were captured on a Nikon Ti-C2plus confocal microscope (Nikon Instr., Lewisville, Texas, USA) using the NIS-Elements AR V.4.20.00 software.

In vitro cytotoxicity assays

The cytotoxicity of CAR T cells was evaluated by bioluminescence imaging (BLI) assays. Luc^+ NET cells (1×10^4/well) were co-cultured for up to 72 hours with either UT T cells or anti-SSTR CAR T cells at an effector:target (E:T) ratio ranging between 10:1 and 1:10. Following the addition of D-Luciferin (Perkin Elmer) at 150 µg/mL, bioluminescence was measured using a Victor X4 plate reader (Perkin Elmer). The percentage of specific tumor cell lysis was determined using the following formula: % lysis=1-(mean BLI signal in the presence of anti-SSTR CAR T cells/mean BLI signal in the presence of UT cells) x 100%. Experiments were carried out in triplicate.

Cytokine release assays

CAR T cells were co-cultured with NET cells at an E:T ratio of 1:1 for 24 hours. The supernatant was then harvested and the concentration of interferon-γ (IFNγ) and tumor necrosis factor alpha (TNF-α) was measured by ELISA (Thermo Fisher Scientific). T cells were activated through CD3/CD28 stimulation (T cell TransAct, Miltenyi) in positive control experiments. T cells were cultured in the absence of tumor cells in negative control experiments.

Fluorescence in situ hybridization

Metaphase spreads and interphase nuclei were obtained from the CM cell line. Fluorescence in situ hybridization (FISH) experiments were performed using probes targeting human *SSTR2* and *SSTR5*. Probes were directly labeled by nick-translation with Cy3-dUTP and fluorescein-dUTP (Enzo Life Sciences, Farmingdale, New York, USA), as described.[17] Nuclei and chromosome metaphases were simultaneously DAPI-stained. Digital images were obtained using a Leica DMRXA2 epifluorescence microscope equipped with a cooled CCD camera (Teledyne Princeton Instruments, Trenton, New Jersey, USA). DAPI, Cy3 and fluorescein fluorescence signals were detected using specific filters and recorded separately as grayscale images. Pseudocoloring and merging of images were performed using Adobe Photoshop software.

CRISPR/Cas9

The CRISPR/Cas9 technology was used to induce frameshift mutations in *SSTR2* and *SSTR5* in CM cells. For each gene, a plasmid co-expressing Cas9, two specifically designed gRNAs (online supplemental table 1) and GFP was purchased from VectorBuilder (Neu-Isenburg, Germany). Sanger sequencing was then carried out to ensure the presence of intact CRISPR targets in Luc^+ CM cells, while FISH was employed to assess the number of *SSTR2* (ABC8-2147740L18 probe) and *SSTR5* (RP11-141G9 probe) alleles. Luc^+ CM cells were co-transfected with the Cas9-containing plasmids and a plasmid comprizing a blasticidin resistance cassette (20:1 molar ratio). PEI-Max 40 000 (Polysciences, Warrington, PA, USA) was used as transfection reagent. The day after the transfection, single cell cultures were prepared and blasticidin was added to the medium to reach a final concentration of 10 µg/mL. GFP^+ single cell clones were then screened by Sanger sequencing for mutations in the gene of interest and the CRISP-ID algorithm was used to genotype all alleles from a single sequencing trace.[18] Clones carrying the mutation of *SSTR2* (CM-$SSTR2^{mut}$),

SSTR5 (CM-SSTR5^{mut}) or both (CM-SSTR2/5^{mut}) were expanded and used for subsequent experiments. Levels of SSTR2 and SSTR5 downstream CRISPR/Cas9 were determined by flow cytometry and real time PCR (RT-PCR), as previously described.[14]

Animal experiments

Sixty-six 4–6 weeks old NOD.Cg-Prkdc^{scid}Il2rg^{tm1Wjl}/SzJ (NSG) female mice (Charles River, Lecco, Italy) were used for adoptive T cell transfer experiments. Briefly, each mouse received a subcutaneous injection of 2×10^6 Luc$^+$-CM or Luc$^+$-BON1 cells resuspended in a 1:1 mixture of HBSS (Euroclone, Milan, Italy) and Matrigel (BD Bioscience). When tumors became palpable, at approximately day 15, mice were randomized to receive 7×10^6 anti-SSTR CAR T cells (n=11), 7×10^6 UT T cells (n=11), or phosphate-buffered saline (PBS) (n=11) via tail vein injection. The number of CAR-transduced CD8$^+$ T cells administered to each mouse was equalized based on ddPCR analysis of CAR vector-positive cells. Following treatment in each group, mice received three daily intraperitoneal administrations of recombinant human IL-2 (Miltenyi Biotec) at 220 000 IU in 500 µL of PBS. Tumor growth was monitored weekly by an observer blinded to treatment allocation via in vivo BLI using an IVIS Lumina SIII instrumentation (Perkin Elmer). The tumor growth rate was quantified as the ratio between total photon flux at each investigational time-point and baseline levels. All animals were euthanized after 4 weeks from treatment, and tumors, brain, pancreas and spleen were harvested, fixed in formalin and embedded in paraffin. We used the ARRIVE checklist when writing our report.[19]

PCR

DNA was extracted from explanted tumors and organs using the DNeasy Blood and Tissue kit (Qiagen). The NanoDrop ND-1000 UV-Vis spectrophotometer (Thermo Fisher Scientific) was employed to quantify the DNA. The presence of the CAR sequence was investigated using the primers listed in online supplemental table 1. PCR reactions were run in triplicate in 20 µL of final volume with 50 ng of sample DNA.

Histopathological analysis

Tumor xenografts and murine SSTR-expressing organs were subjected to H&E staining to reveal pathologic signs of tumor regression or healthy tissue damage. Immunohistochemistry (IHC) was used to assess the expression of the CAR targets using mAbs against SSTR2 (UMB1 clone; 1:5000 dilution) and SSTR5 (UMB4 clone; 1:100 dilution). Sections 4 µm in thickness were stained using the Dako Autostainer according to the manufacturer's instructions. Human pancreatic tissue was used as positive control. The staining was interpreted as positive only when membrane immunoreactivity was detected. Images were acquired using an Eclipse E400 microscope (Nikon Instruments, Melville, New York, USA).

Statistical analysis

Continuous data are expressed as means±SEs. Comparisons between groups were performed using the unpaired Student's t-test, while the Pearson correlation coefficient was calculated for correlation analyses. In vivo tumor growth statistics were calculated using the two-way analysis of variance with Bonferroni post-test based on linear slope of the tumor growth at each data point. All tests were two sided, and a $p<0.05$ was considered statistically significant. Statistical analyses were performed using GraphPad Prism V.5 software (GraphPad Software, La Jolla, California, USA) and MedCalc software V.12.7 (MedCalc Software bvba, Ostend, Belgium). The sample size calculation for animal experiments was performed using MedCalc. Being $\alpha=0.05$, $\beta=80\%$, the droup-out rate=20%, 11 mice per arm were needed to test the null hypothesis (H_0) that anti-SSTR CAR-T cells induce ≤30% tumor bioluminescence regression. All in vitro experiments were repeated at least three times.

RESULTS

Expression of membrane SSTRs by NET cell lines

We examined the expression of membrane SSTR2 and SSTR5 in NET cell lines by WB. As shown in figure 1A, all cell lines expressed the SSTRs, although at variable degrees. These findings were confirmed by flow cytometry and confocal microscopy experiments employing Abs targeting epitopes located in the extracellular portion of SSTRs to detect only potential targets of CAR T therapy (figure 1B,C). No SSTR expression was found by WB, flow cytometry and confocal microscopy in the negative control HAP1 cells (figure 1B and online supplemental figure 1). A summary of % of SSTR positivity and mean fluorescence intensity (MFI) by flow cytometry is provided in table 1. Overall, SSTR2 and SSTR5 were expressed by 35%–70% and 75%–98% of human NET cells, respectively.

Generation of anti-SSTR CAR T cells

We generated a retroviral vector encoding a second-generation CAR comprizing two molecules of octreotide (in tandem) linked to an intracellular signaling domain consisting of human CD28 and CD3ζ via the human CD8 transmembrane region (figure 2A). CD8$^+$ T cells from healthy donors were retrovirally transduced to generate anti-SSTR CAR T cells. As shown in figure 2B, CAR-specific CD3ζ bands could be identified by WB in CAR T cells but not in UT T cells after 2 weeks of expansion. By ddPCR, the percentage of CAR vector-positive T cells was 24% (±6%) at the beginning of the in vitro expansion with IL-2 (day 0), 33% (±9%) at day +14 and 39.5 (±5%) at day +21 (figure 2C,D).

In vitro antitumor activity of anti-SSTR CAR T cells

Anti-SSTR CAR T cells were co-incubated for up to 72 hours with Luc$^+$ NET cell lines. Then, their antitumor activity was measured by in vitro BLI assays. As shown in

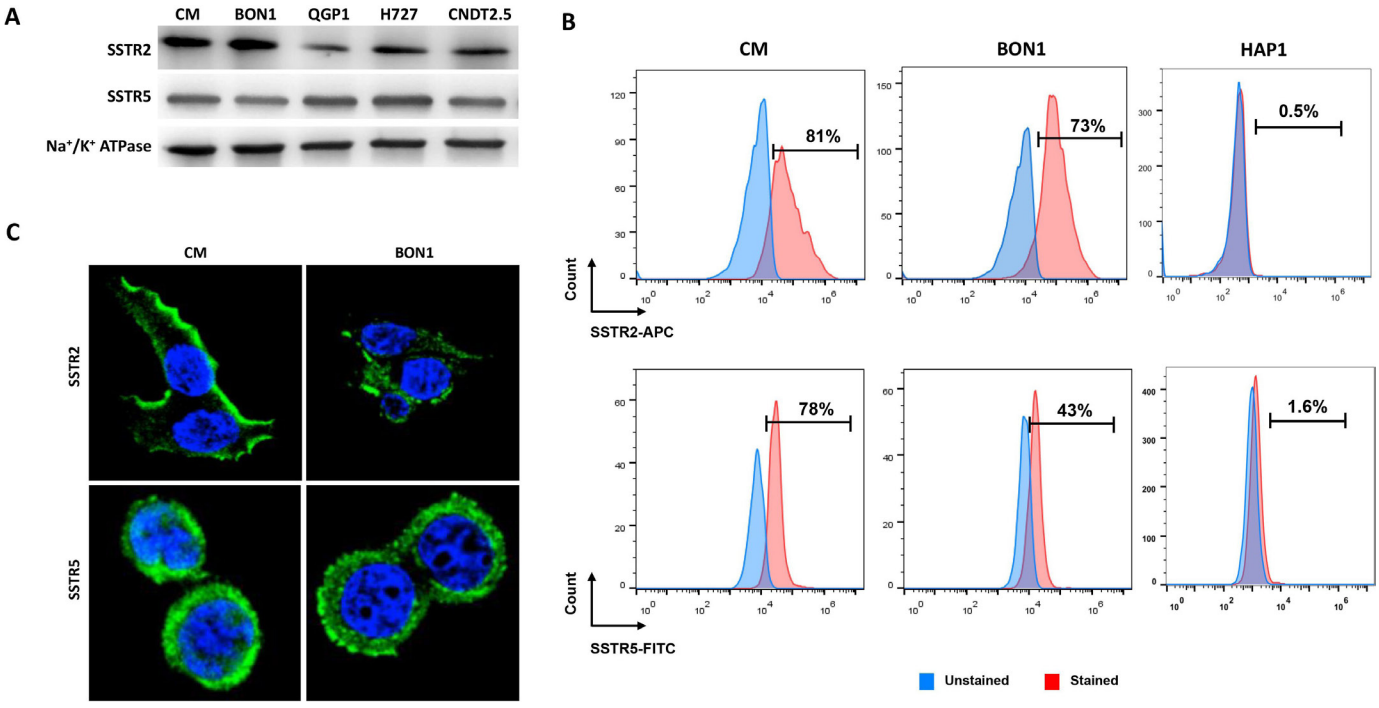

Figure 1 Expression of SSTR2 and SSTR5 by NET cell lines. (A) WB of membrane extracts from CM, BON1, QGP1, H727 and CNDT2.5 cell lines. Na^+/K^+ATPase membrane expression was used as loading control. (B) Representative flow cytometry analysis of SSTR2 and SSTR5 expression in CM and BON1 cells as well as in HAP1 cells as negative control. (C) Representative confocal microscopy evaluation of SSTR2 and SSTR5 expression in CM and BON1 cells. For both flow cytometry and confocal microscopy experiments permeabilization procedures were omitted to allow detection of membrane SSTRs only. SSTRs, somatostatin receptors; WB, Western blot.

figure 3A, the tumoricidal effect of anti-SSTR CAR T cells increased over time and peaked at 72 hours. At an E:T ratio of 1:1, CAR T cells induced cell death in 58% (±8%), 53% (±1%), 42% (±3%), 37% (±7%) and 31% (±14%) of BON1, QGP1, CM, CNDT2.5 and H727 cells, respectively, after 72 hours of co-culture. The levels of tumor cell death increased with increasing E:T ratios (figure 3B). UT T cells induced negligible levels of tumor cell death (<10%), irrespective of target cell line, incubation time and E:T ratios (online supplemental figure 2). To ascertain whether the killing ability of anti-SSTR CAR T cells was paralleled by specific lymphocyte activation and production of effector cytokines, we measured the release of IFN-γ and TNF-α by ELISA after 24 hours co-culture of tumor cells with UT or CAR T cells. As shown in figure 3C,D, anti-SSTR CAR T cells released significantly higher levels of proinflammatory cytokines as compared with UT T cells ($p<0.05$).

Table 1 Expression of membrane SSTR2 and SSTR5 by flow cytometry across cell lines

Cell line	SSTR2 % (±SD)	SSTR2 MFI (±SD)	SSTR5 % (±SD)	SSTR5 MFI (±SD)
BON1	54.6 (±18.3)	1564 (±613)	65.1 (±23.4)	15 379 (±2720)
CM	67.1 (±11.8)	4347 (±2158)	90.4 (±15.3)	22 016 (±6833)
QGP1	69.3 (±18)	3303 (±1120)	92.6 (±2)	21 062 (±4279)
CNDT2.5	34.6 (±13)	1272 (±413)	98 (±1)	26 578 (±6686)
H727	42.7 (±12.4)	1732 (±910)	89.7 (±18.7)	22 107 (±9312)
CM-SSTR2^{KO}	0.9 (±0.4)	575 (±61)	–	–
CM-SSTR5^{KO}	–	–	3.2 (±2.8)	4002 (±2056)
CM-SSTR2/5^{KO}	2.5 (±1.8)	595 (±134)	4.7 (±0.4)	5039 (±956)
Primary lymphocytes	4.3 (±2.7)	596 (±153)	6.4 (±2)	11 193 (±8845)
MIN6	35 (±4.9)	1020 (±411)	41.7 (±10.2)	25 849 (±840)
HAP1	0.5 (±0.5)	476 (±320)	1.5 (±1.1)	1740 (±872)

Experiments were carried out in triplicate.
MFI, mean fluorescence intensity; SSTR, somatostatin receptor.

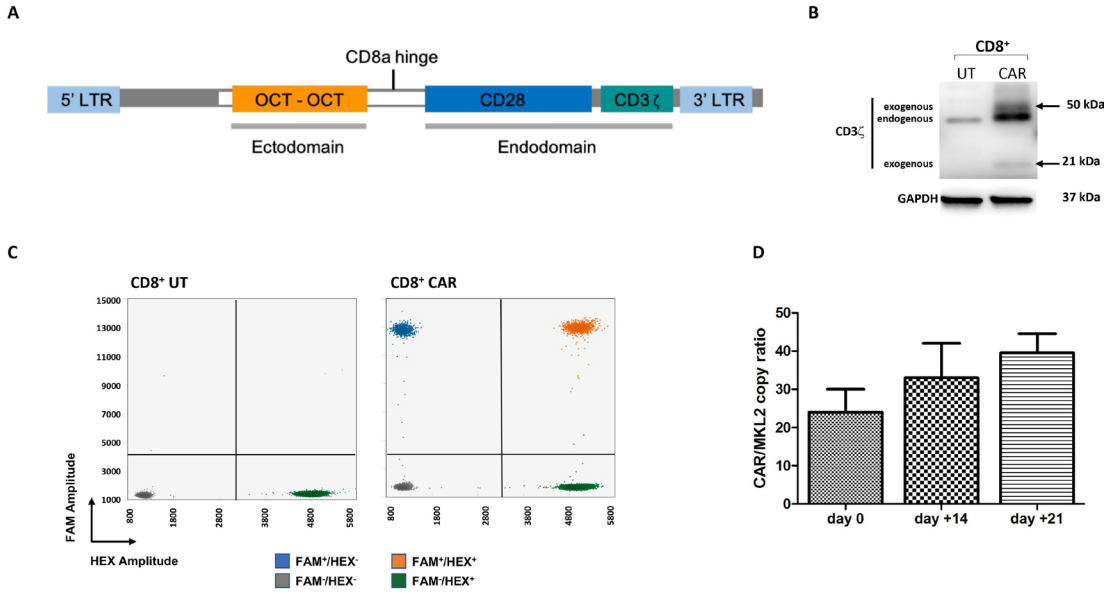

Figure 2 T cells can be engineered to express the anti-SSTR CAR. (A) Diagram of the expression cassette of the second-generation anti-SSTR CAR. The sequence of two molecules of octreotide (OCT) were cloned in frame with CD8aTM, CD28 cytoplasmic moiety and the CD3ζ signaling domain. (B) After 2 weeks from retroviral transduction, 5×10^6 $CD8^+$ T cells from healthy donors were analyzed by WB with an anti-CD3ζ mAb, or an anti-GAPDH mAb as a loading control. The arrows correspond to the CAR-derived p21 and p50 CD3ζ molecules. (C) 2D-amplitude droplet gating of representative ddPCR experiments employing FAM-labeled and HEX-labeled probes against the CAR sequence and the MKL2 reference gene, respectively. The ratio between the FAM^+ droplets corresponding to the CAR sequence (blue +orange fractions) and the HEX^+ droplets corresponding to the housekeeping gene (green +orange fractions) shown here is 0.33. (D) FAM^+/HEX^+ droplet ratio as a surrogate of retroviral transduction efficiency at the beginning of the expansion phase (day 0) and then after 14 and 21 days, respectively. Data from three healthy donors are expressed as average ±SEs. CAR, chimeric antigen receptor; ddPCR, droplet digital PCR; FAM: fluorescein amidite; GAPDH: glyceraldehyde-3-phosphate dehydrogenase; LTR, long terminal repeat; SSTRs, somatostatin receptors; UT, untransduced.

Assessment of CAR T cell killing specificity

To evaluate the specificity of the tumor cell killing induced by anti-SSTR CAR T cells, we induced frameshift mutations in the *SSTR2* and/or *SSTR5* genes in CM cells by CRISPR/Cas9. Three copies of *SSTR2* and *SSTR5*, respectively, were identified by FISH in CM cells, and frameshift mutations or ample deletions were generated in all of them as decoded by CRISP-ID[18] based on Sanger sequencing results (online supplemental figure 3). By RT-PCR, mutant cell lines displayed substantially lower levels of SSTR2/5 transcripts as compared with the parental cell line, in the presence of negligible protein expression (<5%) by flow cytometry (table 1; online supplemental figure 3). When co-cultured with CM-$SSTR2^{mut}$ or CM-$SSTR2/5^{mut}$, CAR T cells did not show any cytolytic potential (figure 3E,F). Limited cytotoxic activity was observed after co-incubation of CAR T cells with CM-$SSTR5^{mut}$ cells for 72 hours, in line with the higher affinity shown by octreotide toward SSTR2. As shown in figure 3G,H, CAR T cells produced lower amounts of proinflammatory cytokines after co-culture with CM-$SSTR2^{mut}$, CM-$SSTR5^{mut}$ and CM-$SSTR2/5^{mut}$ cells with respect to co-incubation with CM cells. Collectively, these data indicate that the tumor cell killing activity displayed by anti-SSTR CAR T cells is highly specific.

In vitro fratricidal activity of anti-SSTR CAR T cells

To rule out the possibility that anti-SSTR CAR T cells could exert fratricidal activity, we examined the expression of SSTR2 and SSTR5 in UT and CAR-engineered T lymphocytes from three different donors by flow cytometry after isolation/transduction (day 0) and then after 24 hours, 72 hours, and 15 days, in the absence or in the presence of CD3/CD28 T cell stimulation via TransAct (online supplemental figure 4). The percentage of $SSTR^+$ T cells did not decline over time, indicating that anti-SSTR CAR T cells do not exert fratricidal activity, even when T cells are activated. Notably, the MFI of SSTR2 in T cells was considerably lower than that recorded in NET cells (table 1, online supplemental figure 4), thus suggesting that a critical density of SSTR2 expression is required to evoke a potent, specific CAR T cell attack.

Antitumor activity of anti-SSTR CAR T cells in vivo

To evaluate whether anti-SSTR CAR T cells could mediate an antitumor response in vivo, we established a murine model of adoptive cell transfer consisting of immunodeficient NSG mice engrafted with two different $SSTR^+$ NET cell lines followed by intravenous infusion of CAR-engineered human T cells, UT T cells, or PBS (figure 4A). Transduced $CD8^+$ lymphocytes were administered together with UT $CD4^+$ T cells to provide homeostatic

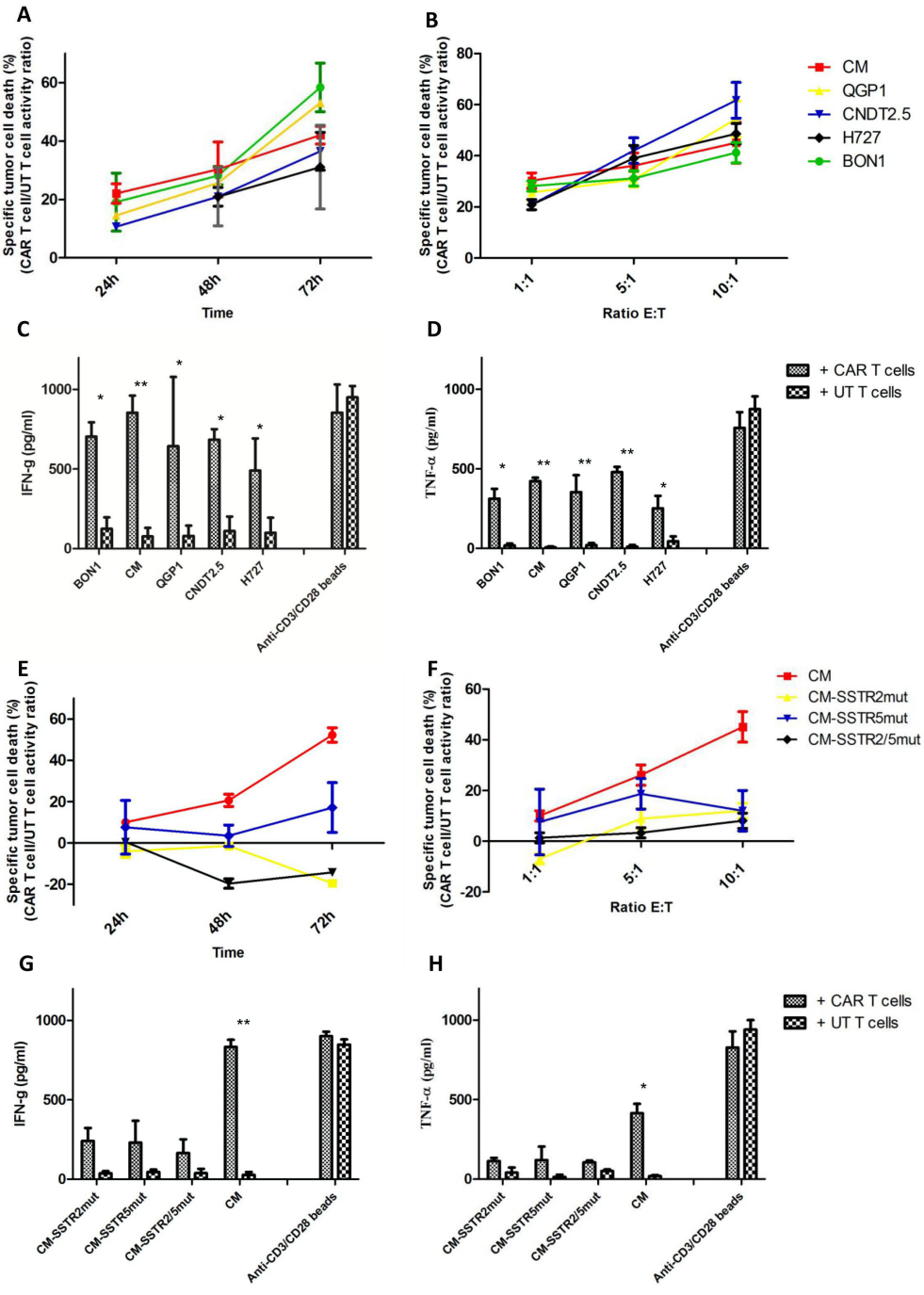

Figure 3 Anti-SSTR CAR T cells exhibit antigen-specific tumoricidal activity. (A) Anti-SSTR CARs endow human T lymphocytes with reactivity against SSTR-expressing targets. By in vitro BLI assay, CAR T cells induced cell death in up to 58% of Luc$^+$ NET cell lines as compared with UT T cells at an E:T ratio of 1:1. The percentage of specific tumor cell lysis was calculated as the ratio between CAR T cell and UT T cell antitumor activity using the formula: % lysis=1-(mean BLI signal in the presence of anti-SSTR CAR T cells/mean BLI signal in the presence of UT cells) x 100%. (B) In vitro BLI assay to evaluate the cytolytic activity of CAR T cells as compared with UT T cells according to increasing E:T ratios after 24 hours of coculture with NET cells. The degree of cytotoxicity induced by CAR T cells increased when the number of effector cells increased. (C) IFN-γ and (D) TNF-α release on 24 hours coculture of NET cells with CAR T cells or UT T cells at an E:T ratio of 1:1. Cytokine production was measured in culture supernatants by ELISA. CD3/CD28 T cell stimulation through TransAct was used for positive control experiments. (E) In vitro BLI assay to investigate the cytolytic activity of CAR T cells as compared with UT T cells against mutant CM cells and parental cells at an E:T ratio of 1:1. (F) Evaluation of the cytotoxic potential of CAR T cells against CM cells harboring wild-type or mutated SSTR2 and/or SSTR5 according to increasing E:T ratios after 24 hours of coculture. (G) IFN-γ and (H) TNF-α release on 24 hours coculture of CAR T cells or UT T cells with mutated or parental CM cells at an E:T ratio of 1:1. All experiments were carried out in technical triplicate using lymphocytes from three healthy donors. Mean values and standard errors are represented in figure. *P<0.05, **p<0.01. CAR, chimeric antigen receptor; E:T, effector:target; NET, neuroendocrine tumor; SSTR, somatostatin receptor; UT, untransduced.

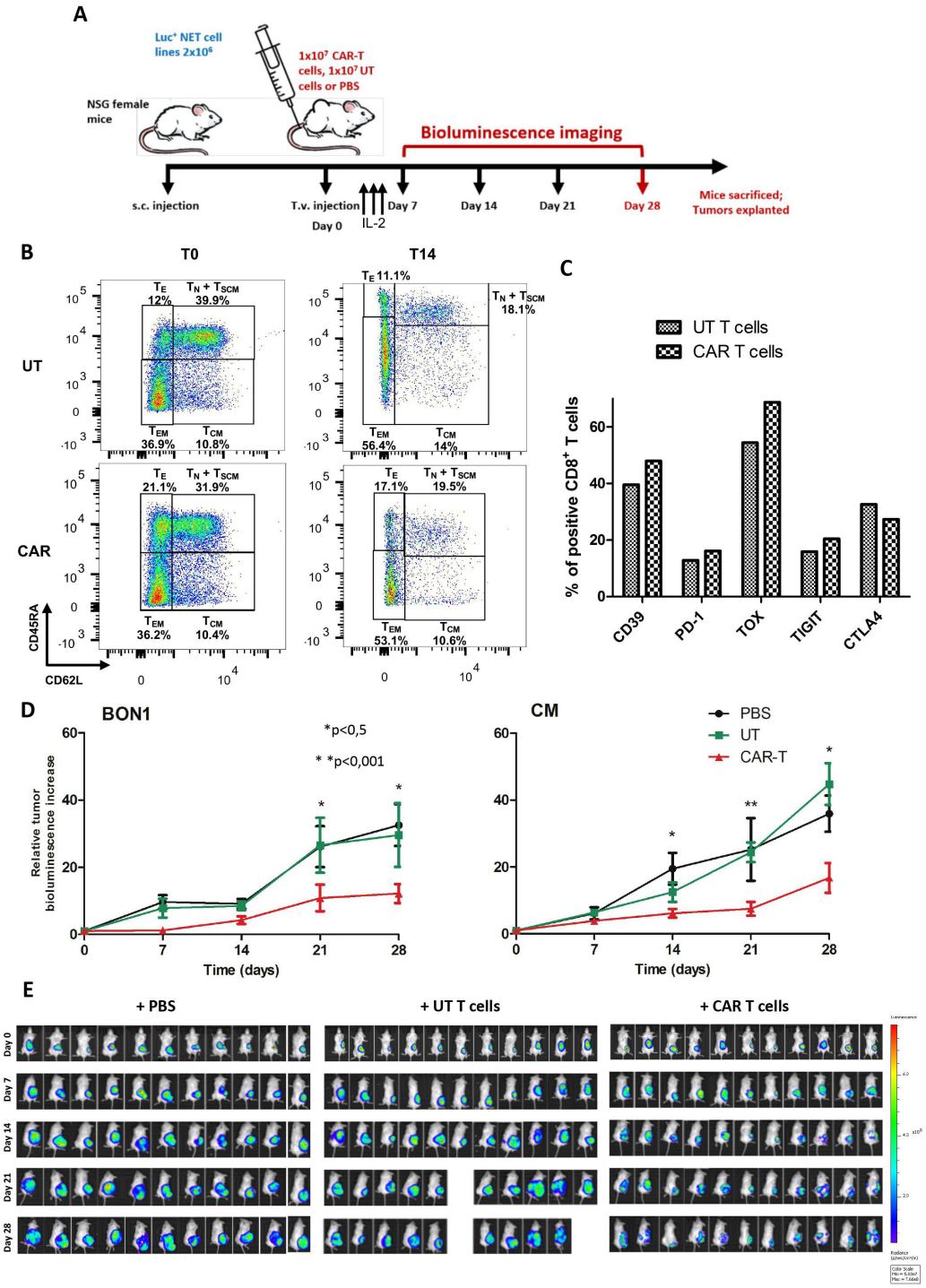

Figure 4 Anti-SSTR CAR T cells effectively inhibit the growth of NET xenografts in vivo. (A) Experimental design of the adoptive cell transfer experiments in the NSG murine model. When the subcutaneous NET xenografts reached 1 mm^3 in volume by caliper measurement, mice were randomized to receive PBS, UT T cells, or anti-SSTR CAR T cells by tail vein injection. Following treatment, mice received three daily intraperitoneal administration of recombinant human IL-2. The response to treatment was assessed once weekly by in vivo BLI, and tumor bioluminescence was normalized to baseline. After 4 weeks from treatment, mice were sacrificed and tumors, brain, pancreas and spleen were explanted. (B) Characterization of the T cell differentiation status of the adoptive products to be infused in mice. The flow plots of UT T cells and CAR T cells at the beginning (T0) and at the end of the ex vivo expansion phase (T14) are represented. (C) Characterization of the expression of exhaustion markers by UT T cells and CAR T cells before injection in mice. (D) Growth curves of BON1 and CM xenografts after treatment with anti-SSTR CAR T cells or UT T cells or PBS. Bioluminescence increase relative to baseline values is expressed as mean of 11 tumor-bearing mice±standard errors. *P<0.05; **p<0.01. (E) Bioluminescence images of NSG mice bearing CM xenografts from day 0 (i.v. infusion of PBS, UT T cells or CAR T cells) to day 28 (end of the experiment). Color scale for all images: min=5x10^7, max 7.7×10^8. CAR, chimeric antigen receptor; PBS: phosphate-buffered saline; SSTR, somatostatin receptor; UT, untransduced.

cytokines as previously described.[20] To characterize the composition of the cellular products infused in mice, both UT and CAR-transduced T lymphocytes were subjected to flow cytometry to determine their differentiation status as well as the expression of exhaustion markers. As shown in figure 4B, the naïve compartment decreased substantially after 14 days of culture with IL-2 in both UT and transduced T cells, in favor of an effector memory phenotype. One day before injection in mice, the percentage of T_N, T_{SCM}, T_{CM}, T_{EM} and T_E cells was 12.6%, 0.2%, 14%, 56.4% and 11.1%, respectively, in UT T cells and 13.4%, 0.5%, 10.6%, 53.1%, and 17.1%, respectively, in CAR T cells (gating strategy shown in online supplemental figure 5). Before infusion, the expression of exhaustion markers such as CD39, PD-1, TOX and TIGIT was slightly higher in CAR T cells as compared with UT T cells (figure 4C). When CM and BON1 xenografts had a mean volume of 1 mm^3, mice were randomized to receive treatments. As shown in figure 4D,E and online supplemental figure 6, mice receiving anti-SSTR CAR T cells exhibited a significant reduction in tumor growth as compared with those treated with UT T cells or PBS ($p<0.05$) by in vivo BLI. In particular, the difference between the three groups became significant after 14 and 21 days from treatment in CM and BON1 xenografts, respectively. No weight loss or abnormal animal behaviors were observed in mice treated with CAR T cells (data not shown).

Target persistence and CAR T cell infiltration of murine xenografts

To evaluate the expression of SSTR2 and SSTR5 in CM and BON1 xenografts, all tumors were explanted after mice sacrifice. By IHC, the expression of SSTR2/5 was revealed in all but three tumors (CM, n=1; BON1, n=2) (figure 5A, online supplemental figure 7). Mice harboring these tumors had all undergone treatment with anti-SSTR CAR T cells. Remarkably, the individual growth rate of these tumors was among the lowest in the whole xenograft cohort (online supplemental figure 7), thus suggesting that this improved tumor control might be the consequence of the eradication of the $SSTR^+$ clones induced by the CAR T treatment. We next sought to investigate whether CAR T cells were able to traffic and infiltrate into tumor xenografts. By PCR, the CAR transgene was identified in all tumors treated with the transduced T cells (figure 5B). We also quantified the degree of CAR T cell infiltration of tumor xenografts using ddPCR, which allows measurement of absolute gene copy number to determine CAR-vector positive cells. As shown in figure 5C, the infiltration of tumors was overall low after 4 weeks of administration, with improved tumor control observed when the number of CAR vector-positive cells was higher ($r=-0.45$; $p=0.04$). No relationship was seen between the extent of tumor necrosis identified by H&E staining and the treatment with CAR T cells, UT T cells or PBS, possibly owing to the inherent formation of necrosis during the growth of NET cell line xenografts as result of the tumoultous proliferation of tumor cells (online supplemental figure 7).

On-target/off-tumor toxicities in the in vivo model

We first assessed the relevance of our in vivo model in the evaluation of potential on-target/off-tumor toxicities. To this aim, we co-incubated human anti-SSTR CAR T cells or UT T cells with the MIN6 cell line, a murine panNET cell line expressing SSTR2/5 (table 1). As shown in figure 5D and online supplemental figure 2, anti-SSTR CAR T cells, but not UT T cells, exhibited a specific tumoricidal activity against MIN6 cells, thus demonstrating that the transduced T cells could recognize the murine isoforms of SSTRs. In line with this observation, anti-SSTR CAR T cells produced significantly higher amounts of IFN-γ than UT T cells when incubated for 24 hours with MIN6 cells (figure 5E). We then investigated whether CAR T cells were able to infiltrate and persist into the murine spleen, pancreas or brain as models of SSTR-expressing organs. PCR experiments demonstrated the presence of the CAR transgene in all explanted organs (figure 5B). Finally, we evaluated the presence of microscopic tissue damage in SSTR-expressing organs. By H&E staining, no obvious damage could be observed in the spleen, pancreas or brain of mice treated with anti-SSTR CAR T cells (figure 5F).

DISCUSSION

The remarkable success of CAR T cell therapy against hematologic malignancies highlights a promising direction to improve cancer immunotherapy. In this study, we evaluated the antitumor activity of CAR T cells targeting $SSTR^+$ NET cell lines in vitro and in vivo. To the best of our knowledge, this is the first report to highlight the possibility of effectively incorporating a synthetic peptide drug within the extracellular moiety of a CAR.

In recent years, immune checkpoint inhibitors (ICIs) have represented a major breakthrough in the treatment of cancer. However, this form of immunotherapy has shown only marginal activity against well-differentiated NETs,[21–24] probably as the result of their low mutational burden, 'cold' immune microenvironment, rare PD-L1 positivity and defective HLA expression.[25–27] While adoptive T cell immunotherapy has the potential to circumvent the hurdles of ICIs, such an approach has never been investigated in NETs so far.

The frequent overexpression of SSTRs by well-differentiated NETs makes this family of receptors an attractive target for CAR T cell therapy. Given that SSTR subtypes may be expressed differently across NETs of different primary sites,[3] the generation of a CAR targeting all or most of the SSTRs appears highly desirable to cover the whole spectrum of NETs. Octreotide is a synthetic octapeptide derived from the human hormone somatostatin and is used to control both secretion and proliferation of NETs in clinical practice since the 1980s. Its cyclic structure is imparted by a naturally

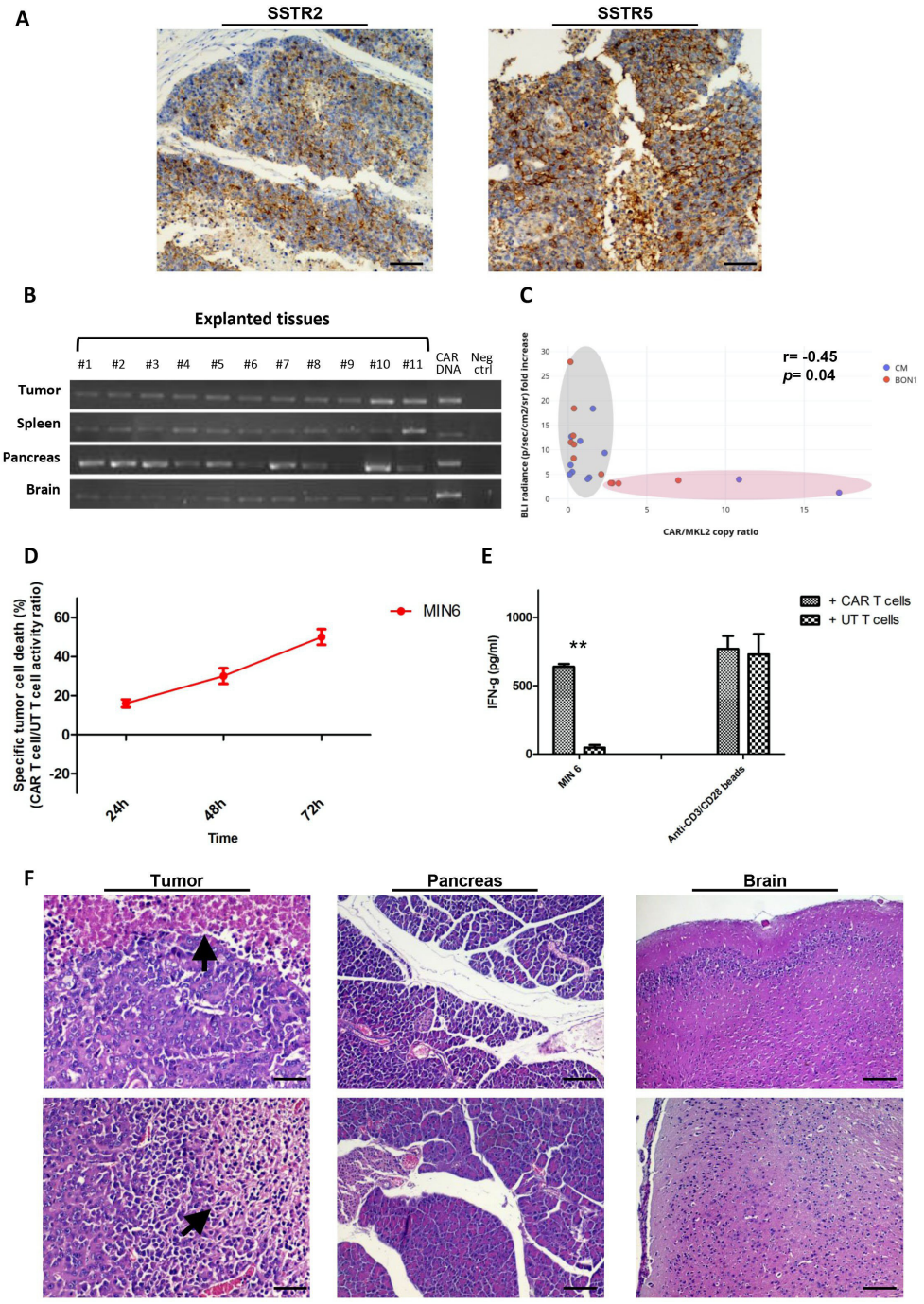

Figure 5 Anti-SSTR CAR T cells infiltrate human xenografts and murine SSTR-expressing organs. (A) Visualization of SSTR2 (UMB1 mAb) and SSTR5 (UMB5 mAb) within tumor xenografts by IHC. Magnification: ×20. Scale bar: 100 µm. (B) Explanted CM tumor xenografts as well as SSTR-expressing organs such as murine spleen, pancreas and brain were lysed and subjected to DNA extraction. The infiltration of CAR T cells was demonstrated by PCR using primers specific for the anti-SSTR CAR sequence. The purified CAR construct DNA was used for positive control experiments. Distilled water was used in negative control experiments. (C) FAM-labeled and HEX-labeled probes against the CAR sequence and the MKL2 reference gene, respectively, were employed in ddPCR experiments to quantify the infiltration of CM (blue dots) and BON1 xenografts (red dots) by anti-SSTR CAR T cells. An inverse correlation can be observed between CAR T cell infiltration and tumor bioluminescence increase relative to baseline. (D) Anti-SSTR CAR T cells recognize and kill the MIN6 cells, a murine NET cell line expressing SSTR2/5. By in vitro BLI, CAR T cells induced cell death in the 48% of Luc^+ MIN6 cells as compared with UT T cells at an E:T ratio of 1:1 after 72 hours of coculture. (E) IFN-γ release on 24 hours coculture of NET cells with CAR T cells or UT T cells at an E:T ratio of 1:1. (F) Histopathological analysis of human NET xenografts and murine pancreas and brain by H&E staining. Extensive necrosis foci could be identified within tumors (arrowhead). Representative microphotographs show the absence of necrosis or other tissue damages in the context of the murine pancreas and brain. Magnification: x20. Scale bar: 100 µm. **P<0.01. CAR, chimeric antigen receptor; ddPCR, droplet digital PCR; E:T, effector:target; IHC, immunohistochemistry; NET, neuroendocrine tumor; SSTR, somatostatin receptor; UT, untransduced.

occuring disulfide bridge between two cysteine residues. Octreotide binds with high affinity to SSTR2 and SSTR5, moderate affinity to SSTR3 and low affinity to SSTR1 and SSTR4.[3] We, therefore, decided to incorporate this SSA in the extracellular domain of a CAR containing CD3ζ and CD28 as stimulatory and costimulatory domains, respectively, to impart target specificity against SSTRs. Notably, while the pharmacophoric sequence of octreotide comprises Phe^{7}-D-Trp^{8}-Lys^{9}-Thr^{10} in the β-turn responsible for interaction with SSTRs, only L- amino acids could be incorporated in our CAR. Nevertheless, prior research demonstrated that, despite increasing the stability of the free compound, the D- conformation does not modify the binding affinities to SSTRs.[28–31] Multiple CAR variants differing in their extracellular portion were preliminarily tested in our study (data not shown), but only one comprizing two octreotide molecules interspaced by a short linker showed structural stability, with CAR-specific bands detectable by WB in transduced T cells. Such a variant, that does not necessarily bind more than one SSTR contemporarily, was therefore chosen for subsequent testing.

We evaluated the efficiency of retroviral transduction by ddPCR and found that approximately one third of transduced T cells incorporated the CAR transgene after 2 weeks from transduction. Owing to the possible incorporation of multiple CAR copies per genome, a possible overestimation of transduction efficiency cannot be excluded in our study. However, emerging evidence indicates that a linear relationship exists between the average CAR copy number per cell measured by ddPCR and the proportion of transduced T cells as measured by flow cytometry.[32–35] In this context, ddPCR allowed us to overcome problems related to results inconsintency commonly observed with poorly characterized Abs (like those commercially available against octreotide) and to keep the construct free of modifications (ie, insertion of tag genes) not compatible with immediate clinical trial testing.

In this study, we demonstrate potent, target-dependent cytotoxicity of anti-SSTR CAR T cells against a variety of NET cell lines characterized by various levels of SSTR2/5 expression. Notably, we show that the antitumor activity is not only antigen-specific, but also parallels the known binding affinity profile of octreotide toward SSTR2 (0.56 nM) and SSTR5 (7 nM),[3] as demonstrated by co-incubation of CAR T cells with CM-SSTR2^{mut} or CM-SSTR5^{mut} cell lines. In this context, the overall decrease of SSTR density determined by SSTR2/5 knockout might play a major role in reducing the effectiveness of anti-SSTR CAR T cells, consistent with prior evidence showing a tight dependency between CAR T cell activity and antigen expression density.[36–40] Nuclear medicine imaging techniques employing radiolabeled somatostatin analogs[1] might be used in the future to determine the therapeutic window[41] of anti-SSTR CAR T cells in humans as well as to preselect the patients most likely to respond to this form of therapy.

Consistent with in vitro findings, adoptive cell transfer of anti-SSTR CAR T cells in NSG mice resulted in a significant inhibition of the human xenograft growth. Although graft-versus-host disease due to allogeneic T cell responses is inevitable in murine models of tumor cell line xenografts, the different tumor growth profile observed in mice treated with UT T cells or CAR T cells indicates that the antitumor effect is primarily target-specific. In this context, halting T cell differentiation throughout the ex vivo expansion of CAR T cells might likely result in an improvement of the cytotoxic potential of the T cell transfer.[42] Indeed, approximately 70% of the CAR T cells infused in our murine model displayed a late differentiated, effector phenotype (T_{EM}+T_{E}). In light of recent evidence showing the emergence of CD4^{+} populations with a repertoire dominated by a small number of clones in leukemia patients with decade-long responses induced by anti-CD19 CAR T cells,[43] we cannot exclude that the transduction of bulk lymphocytes containing both CD4^{+} and CD8^{+} T cells instead of CD8^{+} T cells only might have resulted in improved antitumor control.

The expression of SSTRs is not strictly confined to NETs. The receptors are indeed expressed physiologically by dispersed neuroendocrine cells, primarily in the hypophysis and in the islets of Langherans, as well as in the brain, kidney, spleen and exocrine pancreas.[44] Treatments targeting SSTRs, including those with cytolytic potential,[6] are routinely used in clinical practice, and no relevant toxicities are observed as result of a disrupted function of SSTR-expressing organs.[3 45] Nevertheless, on-target/off-tumor toxicities represent one of the major obstacles associated with the development of new CAR T cell therapies in humans, and fatal events have been ascribed to the specific target recognition in healthy organs.[46] *SSTRs* are highly conserved across species, and a high degree of homology exists between the human and mouse genes (*SSTR2*: 99%; *SSTR5*: 80%).[47 48] Consistent with prior evidence demonstrating that SSAs are able to bind the murine SSTRs,[49 50] we showed that anti-SSTR CAR T cells exerted antitumor activity against murine NET cells in vitro. This implies that our animal model could be relevant in predicting potential on-target/off-tumor toxicities in humans, although species-specific differences in the anatomical distribution of SSTR-expressing cells as well as the mouse immunodeficiency per se should be acknowledged as potential confounders, among many others. Surprisingly, the anti-SSTR CAR T cells displayed no obvious toxicities in the brain and pancreas of treated mice, although the presence of CAR-positive cells was uniformly documented in these organs. Although we are currently unable to provide a mechanistic explanation for such a finding, our observation is in line with that of Smith *et al*,[49] who recently developed a hybrid adeno-associated virus and phage (AAVP) vector displaying octreotide on the viral surface for ligand-directed delivery of TNF to NETs and showed the specific localization of the AAVP in tumorous, but not normal, neuroendocrine glands. The mechanism underlying this surprizing phenomenon

should be further explored, and the differential expression density of SSTRs[51] as well as the specific receptor localization on the membrane of NET cells and normal cells should be investigated.

In summary, this study demonstrates that a biologically active drug can be successfully used as a displayed ligand to impart target specificity to CAR T cells. We chose the octreotide peptide motif as an octapeptide synthesized with natural residues, favorable pharmacological attributes and a very well-established track record for targeted drug delivery to NETs. The framework used here is suitable for other known, short, biologically active drugs capable of directing CAR T cells toward their target. The results of this study constitute the first report concerning CAR T cells redirected to SSTRs. Given their antitumor potential and apparently safe toxicity profile, anti-SSTR CAR T cells could be a promising therapeutic option for NETs. The availability of nuclear medicine imaging techniques using radiolabeled octreotide to characterize the expression of SSTRs in human NETs could be used to predict responses to anti-SSTR CAR T cells in patients. Strategies involving the optimization of the efficacy and the enhancement of the persistence of the anti-SSTR CAR T cells (ie, through testing of different costimulatory domains or use of culture conditions less likely to promote T cell terminal differentiation[52]) as well as the inclusion of suicide gene safety switches to render this therapeutic approach safer may be devised to capitalize on the described antitumor activity of the anti-SSTR CAR.

Author affiliations
[1]Department of Interdisciplinary Medicine, University of Bari "Aldo Moro", Bari, Italy
[2]Division of Medical Oncology, Azienda Ospedaliero-Universitaria Consorziale Policlinico di Bari, Bari, Italy
[3]Department of Biology, University of Bari "Aldo Moro", Bari, Italy
[4]Department of Emergency and Organ Transplantation, University of Bari "Aldo Moro", Bari, Italy
[5]Departments of Immunology and Cutaneous Oncology, Moffitt Cancer Center, Tampa, Florida, USA
[6]Department of GI Oncology, Moffitt Cancer Center, Tampa, Florida, USA

Twitter Gerardo Cazzato @Gerardo Cazzato pathologist

Contributors MC, DA-D, JS conceived the work, BM, EP, FM, AP, GC, MCR, performed the experiments and analyzed the data, All authors contributed to the interpretation of results, BM, EP, AP, MC have drafted the article. All authors have critically revised the text. MC is responsible of the overall content as the guarantor.

Funding This work was supported by the Associazione Italiana per la Ricerca sul Cancro (MFAG #23583), European Neuroendocrine Tumor Society (ENETS CoE Excellence Academy Fellowship Grant 2017), Regione Puglia (Research for Innovation – POR Puglia FESR-FSE 2014/2020, REFIN B39303C8) and Associazione per la Ricerca Biomolecolare Onlus, Acquaviva, Italy (2020). Authors thank Nada Chaoul, Raffaele Palmirotta, Paola Cafforio, Federica Cavallo and Krisztian Belenyesi for technical assistance and critical discussion.

Competing interests JS: Ipsen speaker's bureau. DA-D is a member of the Scientific Advisory Board of Anixa Biosciences, and receives research funding support from Intellia Therapeutics and bluebird bio. MCR, JS, DA-D and MC are listed as inventors or co-inventors in patent applications filed by Moffitt Cancer Center, involving adoptive immunotherapy products. Other Authors declare no conflicts of interest.

Patient consent for publication Not applicable.

Ethics approval This study involves human participants and was approved by Ethics Committee National Cancer Institute 'Giovanni Paolo II', Bari (932/CE) Participants gave informed consent to participate in the study before taking part. All procedures were approved by the University of Bari animal care and use committee and the Italian Ministry of Health (authorization n. 810/2020-PR).

Provenance and peer review Not commissioned; externally peer reviewed.

Data availability statement Data are available on reasonable request. All data relevant to the study are included in the article or uploaded as online supplemental information.

ORCID iDs
Barbara Mandriani http://orcid.org/0000-0002-4139-0602
Gerardo Cazzato http://orcid.org/0000-0003-0325-4316

REFERENCES

1 Cives M, Strosberg JR. Gastroenteropancreatic neuroendocrine tumors. *CA Cancer J Clin* 2018;68:471–87.
2 Dasari A, Shen C, Halperin D, *et al*. Trends in the incidence, prevalence, and survival outcomes in patients with neuroendocrine tumors in the United States. *JAMA Oncol* 2017;3:1335–42.
3 Cives M, Strosberg J. The expanding role of somatostatin analogs in gastroenteropancreatic and lung neuroendocrine tumors. *Drugs* 2015;75:847–58.
4 Rinke A, Müller H-H, Schade-Brittinger C, *et al*. Placebo-controlled, double-blind, prospective, randomized study on the effect of octreotide LAR in the control of tumor growth in patients with metastatic neuroendocrine midgut tumors: a report from the PROMID Study Group. *J Clin Oncol* 2009;27:4656–63.
5 Caplin ME, Pavel M, Ćwikła JB, *et al*. Lanreotide in metastatic enteropancreatic neuroendocrine tumors. *N Engl J Med* 2014;371:224–33.
6 Strosberg J, El-Haddad G, Wolin E, *et al*. Phase 3 trial of 177Lu-dotatate for midgut neuroendocrine tumors. *N Engl J Med* 2017;376:125–35.
7 June CH, O'Connor RS, Kawalekar OU, *et al*. CAR T cell immunotherapy for human cancer. *Science* 2018;359:1361–5.
8 Neelapu SS, Locke FL, Bartlett NL, *et al*. Axicabtagene ciloleucel CAR T-cell therapy in refractory large B-cell lymphoma. *N Engl J Med* 2017;377:2531–44.
9 Locke FL, Miklos DB, Jacobson CA. All ZUMA-7 investigators and contributing Kite members. Axicabtagene Ciloleucel as second-line therapy for large B-cell lymphoma. *N Engl J Med* 2021
10 Schuster SJ, Bishop MR, Tam CS, *et al*. Tisagenlecleucel in adult relapsed or refractory diffuse large B-cell lymphoma. *N Engl J Med* 2019;380:45–56.
11 Raje N, Berdeja J, Lin Y, *et al*. Anti-BCMA CAR T-cell therapy bb2121 in relapsed or refractory multiple myeloma. *N Engl J Med* 2019;380:1726–37.
12 Wang M, Munoz J, Goy A, *et al*. KTE-X19 CAR T-cell therapy in relapsed or refractory mantle-cell lymphoma. *N Engl J Med* 2020;382:1331–42.
13 Abate-Daga D, Davila ML. CAR models: next-generation CAR modifications for enhanced T-cell function. *Mol Ther Oncolytics* 2016;3:16014.
14 Cives M, Quaresmini D, Rizzo FM, *et al*. Osteotropism of neuroendocrine tumors: role of the CXCL12/ CXCR4 pathway in promoting EMT in vitro. *Oncotarget* 2017;8:22534–49.
15 Abate-Daga D, Lagisetty KH, Tran E, *et al*. A novel chimeric antigen receptor against prostate stem cell antigen mediates tumor destruction in a humanized mouse model of pancreatic cancer. *Hum Gene Ther* 2014;25:1003–12.

16 Li D, Li N, Zhang Y-F, *et al*. Persistent polyfunctional chimeric antigen receptor T cells that target glypican 3 eliminate orthotopic hepatocellular carcinomas in mice. *Gastroenterology* 2020;158:2250–65.
17 Lichter P, Ward DC. Is non-isotopic in situ hybridization finally coming of age? *Nature* 1990;345:93–4.
18 Dehairs J, Talebi A, Cherifi Y, *et al*. CRISP-ID: decoding CRISPR mediated indels by Sanger sequencing. *Sci Rep* 2016;6:28973.
19 Percie du Sert N, Hurst V, Ahluwalia A. The ARRIVE guidelines 2.0: updated guidelines for reporting animal research.
20 Gattinoni L, Lugli E, Ji Y, *et al*. A human memory T cell subset with stem cell-like properties. *Nat Med* 2011;17:1290–7.
21 Strosberg J, Mizuno N, Doi T, *et al*. Efficacy and safety of pembrolizumab in previously treated advanced neuroendocrine tumors: results from the phase II KEYNOTE-158 study. *Clin Cancer Res* 2020;26:2124–30.
22 Yao JC, Strosberg J, Fazio N, *et al*. Spartalizumab in metastatic, well/poorly-differentiated neuroendocrine neoplasms. *Endocr Relat Cancer* 2021:ERC-20-0382.R1
23 Patel SP, Othus M, Chae YK, *et al*. A phase II basket trial of dual anti-CTLA-4 and anti-PD-1 blockade in rare tumors (dart SWOG 1609) in patients with nonpancreatic neuroendocrine tumors. *Clin Cancer Res* 2020;26:2290–6.
24 Klein O, Kee D, Markman B, *et al*. Immunotherapy of ipilimumab and nivolumab in patients with advanced neuroendocrine tumors: a subgroup analysis of the CA209-538 clinical trial for rare cancers. *Clin Cancer Res* 2020;26:4454–9.
25 Marabelle A, Fakih M, Lopez J, *et al*. Association of tumour mutational burden with outcomes in patients with advanced solid tumours treated with pembrolizumab: prospective biomarker analysis of the multicohort, open-label, phase 2 KEYNOTE-158 study. *Lancet Oncol* 2020;21:1353–65.
26 Puccini A, Poorman K, Salem ME, *et al*. Comprehensive genomic profiling of gastroenteropancreatic neuroendocrine neoplasms (GEP-NENs). *Clin Cancer Res* 2020;26:5943–51.
27 Cives M, Pelle' E, Quaresmini D, *et al*. The tumor microenvironment in neuroendocrine tumors: biology and therapeutic implications. *Neuroendocrinology* 2019;109:83–99.
28 Arison BH, Hirschmann R, Veber DF. Inferences about the conformation of somatostatin at a biologic receptor based on NMR studies. *Bioorg Chem* 1978;7:447–51.
29 Rivier J, Brown M, Vale W. D-Trp8-somatostatin: an analog of somatostatin more potent than the native molecule. *Biochem Biophys Res Commun* 1975;65:746–51.
30 Veber DF, Holly FW, Paleveda WJ, *et al*. Conformationally restricted bicyclic analogs of somatostatin. *Proc Natl Acad Sci U S A* 1978;75:2636–40.
31 Ovadia O, Greenberg S, Laufer B, *et al*. Improvement of drug-like properties of peptides: the somatostatin paradigm. *Expert Opin Drug Discov* 2010;5:655–71.
32 Lu A, Liu H, Shi R, *et al*. Application of droplet digital PCR for the detection of vector copy number in clinical CAR/TCR T cell products. *J Transl Med* 2020;18:191.
33 Haderbache R, Warda W, Hervouet E, *et al*. Droplet digital PCR allows vector copy number assessment and monitoring of experimental CAR T cells in murine xenograft models or approved CD19 CAR T cell-treated patients. *J Transl Med* 2021;19:265.
34 Sugimoto H, Chen S, Minembe J-P, *et al*. Insights on droplet digital PCR-based cellular kinetics and biodistribution assay support for CAR-T cell therapy. *Aaps J* 2021;23:36.
35 Mika T, Maghnouj A, Klein-Scory S, *et al*. Digital-droplet PCR for quantification of CD19-directed CAR T-cells. *Front Mol Biosci* 2020;7:84.
36 Majzner RG, Rietberg SP, Sotillo E, *et al*. Tuning the antigen density requirement for CAR T-cell activity. *Cancer Discov* 2020;10:702–23.
37 Majzner RG, Theruvath JL, Nellan A, *et al*. CAR T cells targeting B7-H3, a pan-cancer antigen, demonstrate potent preclinical activity against pediatric solid tumors and brain tumors. *Clin Cancer Res* 2019;25:2560–74.
38 Watanabe K, Terakura S, Martens AC, *et al*. Target antigen density governs the efficacy of anti-CD20-CD28-CD3 ζ chimeric antigen receptor-modified effector CD8+ T cells. *J Immunol* 2015;194:911–20.
39 Walker AJ, Majzner RG, Zhang L, *et al*. Tumor antigen and receptor densities regulate efficacy of a chimeric antigen receptor targeting anaplastic lymphoma kinase. *Mol Ther* 2017;25:2189–201.
40 Majzner RG, Ramakrishna S, Yeom KW, *et al*. GD2-CAR T cell therapy for H3K27M-mutated diffuse midline gliomas. *Nature* 2022;603:934–41.
41 Watanabe K, Kuramitsu S, Posey AD, *et al*. Expanding the therapeutic window for CAR T cell therapy in solid tumors: the knowns and unknowns of CAR T cell biology. *Front Immunol* 2018;9:2486.
42 Martinez M, Moon EK. CAR T cells for solid tumors: new strategies for finding, infiltrating, and surviving in the tumor microenvironment. *Front Immunol* 2019;10:128.
43 Melenhorst JJ, Chen GM, Wang M, *et al*. Decade-long leukaemia remissions with persistence of $CD4^+$ CAR T cells. *Nature* 2022;602:503–9.
44 Lamberts SW, van der Lely AJ, de Herder WW, *et al*. Octreotide. *N Engl J Med* 1996;334:246–54.
45 Cives M, Strosberg J. Radionuclide therapy for neuroendocrine tumors. *Curr Oncol Rep* 2017;19:9.
46 Morgan RA, Yang JC, Kitano M, *et al*. Case report of a serious adverse event following the administration of T cells transduced with a chimeric antigen receptor recognizing ERBB2. *Mol Ther* 2010;18:843–51.
47 Yamada Y, Post SR, Wang K, *et al*. Cloning and functional characterization of a family of human and mouse somatostatin receptors expressed in brain, gastrointestinal tract, and kidney. *Proc Natl Acad Sci U S A* 1992;89:251–5.
48 Moldovan S, DeMayo F, Brunicardi FC. Cloning of the mouse SSTR5 gene. *J Surg Res* 1998;76:57–60.
49 Smith TL, Yuan Z, Cardó-Vila M, *et al*. AAVP displaying octreotide for ligand-directed therapeutic transgene delivery in neuroendocrine tumors of the pancreas. *Proc Natl Acad Sci U S A* 2016;113:2466–71.
50 Quinn TJ, Yuan Z, Adem A, *et al*. Pasireotide (SOM230) is effective for the treatment of pancreatic neuroendocrine tumors (PNETs) in a multiple endocrine neoplasia type 1 (MEN1) conditional knockout mouse model. *Surgery* 2012;152:1068–77.
51 Majzner RG, Rietberg SP, Sotillo E, *et al*. Tuning the antigen density requirement for CAR T-cell activity. *Cancer Discov* 2020;10:702–23.
52 Meyran D, Terry RL, Zhu JJ, *et al*. Early-phenotype CAR-T cells for the treatment of pediatric cancers. *Ann Oncol* 2021;32:1366–80.